



PERGAMON

Available online at [www.sciencedirect.com](http://www.sciencedirect.com)

SCIENCE @ DIRECT®

International Journal of  
**HEAT and MASS  
TRANSFER**

International Journal of Heat and Mass Transfer 46 (2003) 1725–1735

[www.elsevier.com/locate/ijhmt](http://www.elsevier.com/locate/ijhmt)

# Mixed convection within a porous heat generating horizontal annulus

Khalil Khanafer<sup>a,\*</sup>, Ali J. Chamkha<sup>b</sup>

<sup>a</sup> *Mechanical Engineering Department, University of California, Riverside, CA 92510, USA*

<sup>b</sup> *Mechanical Engineering Department, Kuwait University, Safat 13060, Kuwait*

Received 22 August 2002; received in revised form 16 November 2002

## Abstract

A numerical investigation of mixed convection in a horizontal annulus filled with a uniform fluid-saturated porous medium in the presence of internal heat generation is carried out. The inner cylinder is heated while the outer cylinder is cooled. The forced flow is induced by the cold outer cylinder rotating at a constant angular velocity. The flow field is modeled using a generalized form of the momentum equation that accounts for the presence of porous medium viscous, Darcian and inertial effects. Discretization of the governing equations is achieved using a finite element scheme based on the Galerkin method of weighted residuals. Comparisons with previous works are performed and the results show excellent agreement. The effects of pertinent parameters such as the internal Rayleigh number, the Darcy number, the annulus gap, and the Richardson number on the flow and heat transfer characteristics are considered in the present study. The obtained results depict that the Richardson number plays a significant role on the heat transfer characterization within the annulus. The present results show that an increase in Reynolds number has a significant effect on the flow patterns within the annulus with respect to two-eddy, one-eddy and no-eddy flows. Categorization of the flow regimes according to the number of eddies is established on the  $Ra-Re$  plane for various Rayleigh numbers.

© 2003 Elsevier Science Ltd. All rights reserved.

*Keywords:* Heat generation; Horizontal annulus; Mixed convection and porous medium

## 1. Introduction

Mixed convection heat transfer in an annulus between heated rotating horizontal concentric cylinders has received attention by various investigators in recent years. The motivation for these studies is derived from their technological applications such as cooling of turbine rotors, cooling of high speed gas bearings, the flow condensers for sea water distillation [1], and in the chemical vapor deposition processes for the semiconductor device fabrication. The fluid flow and heat transfer processes within the annulus are controlled by

the combined effects of inertia, buoyancy and centrifugal forces. The resultant effect of these determines the flow pattern and the heat transfer mechanism through the Grashof number and the rotational Reynolds number, respectively. Of particular relevance for this problem is the ratio of the Grashof number to the Reynolds number, which is termed as the Richardson number. This ratio indicates the importance of the buoyancy and the rotational effects on the fluid flow and heat transfer phenomenon within the annulus.

DiPrima and Swinney [2] conducted a comprehensive review of the analytical and experimental studies for flow between concentric rotating cylinders. The interaction of centrifugal and buoyancy forces in a three dimensional horizontal annulus with a heated rotating inner cylinder was studied by Yang and Farouk [1]. In this study, the authors showed that the resulting flows were fully three dimensional for cases where the

\* Corresponding author. Tel.: +1-909-787-6428; fax: +1-909-787-2899.

E-mail address: [khanafer@engr.ucr.edu](mailto:khanafer@engr.ucr.edu) (K. Khanafer).

### Nomenclature

$e_r, e_\phi$	unit vectors in the radial and angular directions, respectively.
$Da$	Darcy number, $\kappa/(r_o - r_i)^2$
$F$	geometric function
$\vec{g}$	gravitational acceleration vector, $\text{m s}^{-2}$
$k$	thermal conductivity, $\text{W m}^{-1} \text{K}$
$\overline{Nu}$	average Nusselt number
$P$	dimensionless pressure, $\text{N m}^{-2}$
$Pr$	Prandtl number, $\nu/\alpha$
$q'''$	volumetric heat generation, $\text{W m}^{-3}$
$r_i$	inner cylinder radius, m
$r_o$	outer cylinder radius, m
$Ra$	Rayleigh number, $g\beta\Delta T(r_o - r_i)^3/\nu\alpha$
$Ra_1$	internal Rayleigh number, $g\beta q'''(r_o - r_i)^5/\nu\alpha k$
$Re$	Reynolds number, $r_o\omega(r_o - r_i)/\nu$
$R_1$	Richardson number, $Ra/PrRe^2$
$t$	time, s
$T$	temperature, $^\circ\text{C}$
$T_r$	nondimensional torque acting on the outer cylinder
$T_{\text{Couette}}$	torque obtained with the Couette velocity distribution, N m
$u, v$	nondimensional velocity components in the radial and angular directions, respectively, $\text{m s}^{-1}$
$\mathbf{u}$	velocity vector, $\text{m s}^{-1}$
$x, y$	Cartesian coordinates, m
$X, Y$	dimensionless coordinates

### Greek symbols

$\alpha$	thermal diffusivity, $\text{m}^2 \text{s}^{-1}$
$\beta$	thermal expansion coefficient $\text{m K}^{-1}$
$\rho_o$	density at reference temperature, $\text{kg m}^{-3}$
$\varepsilon$	porosity
$\phi$	angular coordinate
$\Gamma$	net circulation of the fluid, $ \Psi_o - \Psi_i $
$\kappa$	permeability, $\text{m}^2$
$\psi$	stream function, $\text{m}^2 \text{s}^{-1}$
$\Psi$	nondimensional stream function, $\psi/(r_o - r_i)\omega r_o$
$\Psi_i$	value of the stream function at the inner cylinder
$\Psi_o$	value of the stream function at the outer cylinder
$\omega$	angular velocity, $\text{s}^{-1}$
$\Omega$	nondimensional angular velocity, $\omega(r_o - r_i)/\omega r_o$
$\sigma$	ratio of the inner cylinder diameter to the gap width, $2r_i/(r_o - r_i)$
$\theta$	dimensionless temperature, $(T - T_o)/(T_i - T_o)$
$\tau$	dimensionless time, $t\omega r_o/(r_o - r_i)$
$\nu$	kinematic viscosity, $\text{m}^2 \text{s}^{-1}$

### Subscripts

i	inner cylinder
o	outer cylinder

rotational instability triggered the formation of Taylor cells. Fusegi et al. [3] performed a numerical study for a two-dimensional mixed convection within a horizontal concentric annulus with a heated rotating inner cylinder. The three-dimensional linear stability of the steady mixed convection flow in a moderately wide gap annulus between concentric horizontal cylinders with a heated rotating inner cylinder was studied numerically by Choi and Kim [4]. The results of this study illustrated that the heating of the inner cylinder delayed the formation of Taylor vortices when the effect of rotation dominated the buoyancy effect. Moreover, the results showed that when the effect of buoyant forces predominated over the effect of the centrifugal forces, the rotation of the inner cylinder stabilized the natural convection flow within the horizontal annulus. Lee [5] carried a numerical investigation to determine the temperature and flow patterns of a fluid bounded by two horizontal isothermal concentric and eccentric cylinders. The author showed in this investigation that the average Nusselt number increased with Rayleigh number for both concentric and eccentric

cylinders. Moreover, for a fixed Rayleigh number, the average Nusselt number decreased throughout the flow for an inner rotating cylinder. Yoo [6] investigated numerically the effect of the cooled rotating outer cylinder on the mixed convection of air between two horizontal concentric cylinders. The results demonstrated that the flow patterns could be categorized into three basic types according to the number of eddies: two-eddy, one-eddy, and no-eddy flows. In addition, their results illustrated that the overall heat transfer at the wall decreased as the Reynolds number approached the transitional Reynolds number between the two- and one-eddy flows.

Buoyancy-driven flow and heat transfer between horizontal concentric cylinders filled with a porous medium has been the subject of many investigations in recent years. This is due to the significance of such geometry in a number of engineering applications such as thermal insulation, thermal storage systems, nuclear reactors, underground electrical transmission lines, etc. [7]. Caltagirone [8,9] conducted an extensive analysis of steady-state natural convection in an annulus filled with

a porous medium. Both a perturbation method and a finite difference technique were used to solve the two-dimensional governing equations. A fluctuating three-dimensional regime in the upper part of the porous layer was observed even though the lower part remained strictly two-dimensional. In a related work, Burns and Tien [10] investigated natural convection in concentric spheres and horizontal cylinders filled with a porous medium. Rao et al. [11,12] solved the Boussinesq equations in both two and three dimensions using the Galerkin method. The authors in these studies obtained three possible numerical solutions depending on the initial conditions for a radius ratio of 2 and for Rayleigh numbers above 65. Pop et al. [13] analyzed analytically transient natural convection in a horizontal concentric annulus filled with a porous medium. The inner and outer cylinders were maintained at uniform temperatures. Asymptotic solutions for the inner layer, the outer layer, and the core were obtained for small times. The authors found that, for relatively high Rayleigh numbers, the core was stratified and not isothermal. Stewart and Burns [14] investigated numerically the effects of a permeable inner boundary on the maximum temperature and the convective flows for a two-dimensional horizontal annulus containing a uniformly heat generating porous media. The results of that study illustrated that multi-cellular flows occurred at the highest Rayleigh numbers investigated. In addition, inverted symmetry in flow patterns and temperature distributions happened when the heated isothermal wall condition changed from one cylinder wall to another. Recently, Charrier-Mojtabi [7] conducted a numerical investigation of two- and three-dimensional free convection flows in a saturated porous horizontal annulus heated from the inner surface using a Fourier-Galerkin approximation for the periodic azimuthal and axial directions and a collocation-Chebyshev approximation in the confined radial direction. Bifurcation points between two-dimensional uni-cellular flows and either two-dimensional multi-cellular or three-dimensional flows were determined numerically.

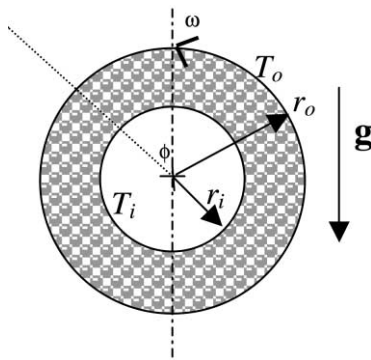


Fig. 1. Schematic of the physical model and coordinate system.

To the best knowledge of the authors, no attention has been given to the problem of mixed convection flow within a horizontal concentric annulus filled with a porous medium for a cooled rotating outer cylinder with internal heat generation. The present study is focused on the analysis of the fluid flow and heat transfer within the annulus using a generalized form of the momentum equation that accounts for the porous medium viscous,

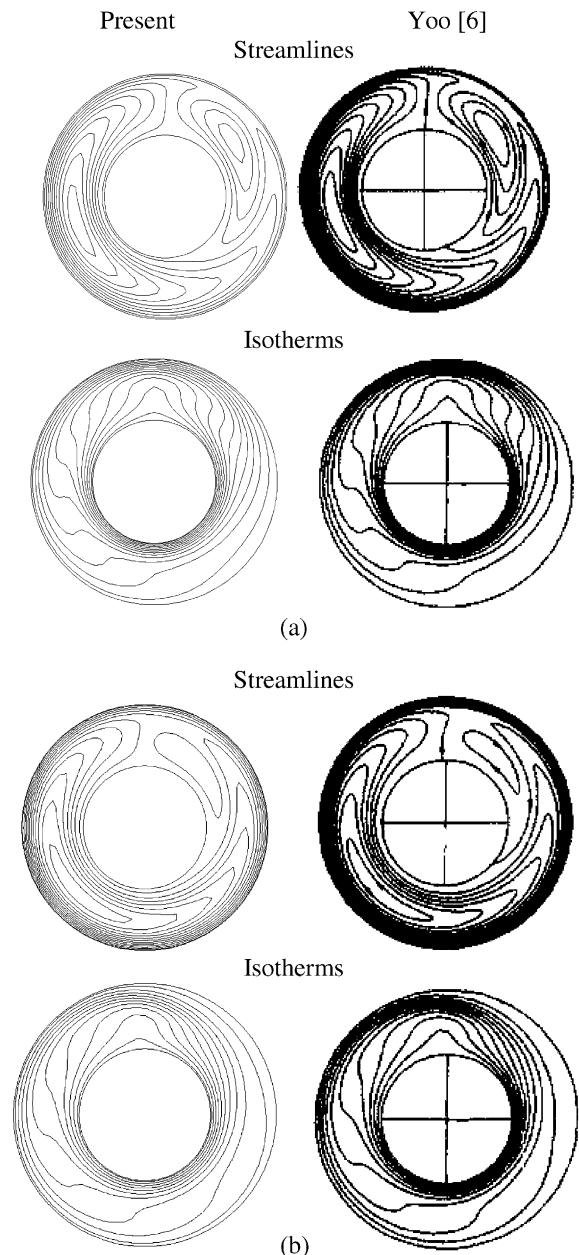


Fig. 2. Comparison of the streamlines and isotherms between the present solution and that of Yoo [6]: (a)  $Re = 100$  and  $Ra = 10^4$  and (b)  $Re = 200$  and  $Ra = 10^4$ .

Darcian and inertial effects. In addition, the effect of the of the forced flow induced by the cooled rotating outer cylinder on the characteristics of buoyancy-driven flow and heat transfer in a porous layer is considered in the present study. The effects of pertinent parameters such as the internal Rayleigh number, Reynolds number, Richardson number, Darcy number, and the ratio of the diameter of the inner cylinder to the annulus width on the flow and heat transfer characteristics are investigated in the present study.

**2. Problem formulation**

The problem under investigation is a laminar two-dimensional mixed-convective flow and heat transfer in

an infinitely long horizontal annulus between two concentric cylinders filled with a uniform fluid-saturated porous medium in the presence of internal heat generation. The geometry of the problem and the coordinate system are shown in Fig. 1. The inner cylinder of radius  $r_i$  and the outer cylinder of radius  $r_o$  are kept at uniform and constant temperatures  $T_i$  and  $T_o$ , respectively, with  $T_i > T_o$ . The inner cylinder is fixed, while the outer cooled cylinder is rotating in the counter-clockwise direction with a constant angular velocity  $\omega$ . The porous medium of porosity  $\varepsilon$  and permeability  $\kappa$  is saturated with an incompressible Newtonian fluid. Viscous heat dissipation in the fluid is assumed to be negligible in comparison to conduction and convection heat transfer effects. It is assumed in the analysis that the thermo-physical properties of the fluid are independent of tem-

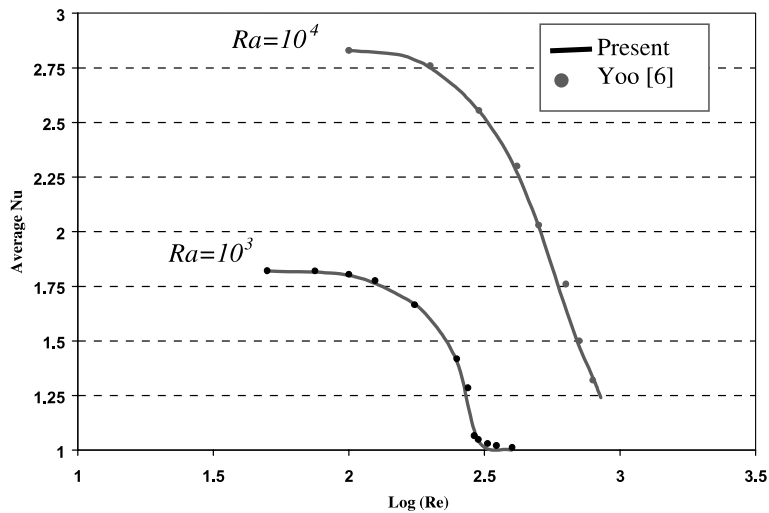


Fig. 3. Comparison of the average Nusselt number for various Reynolds numbers ( $\sigma = 2$ ).

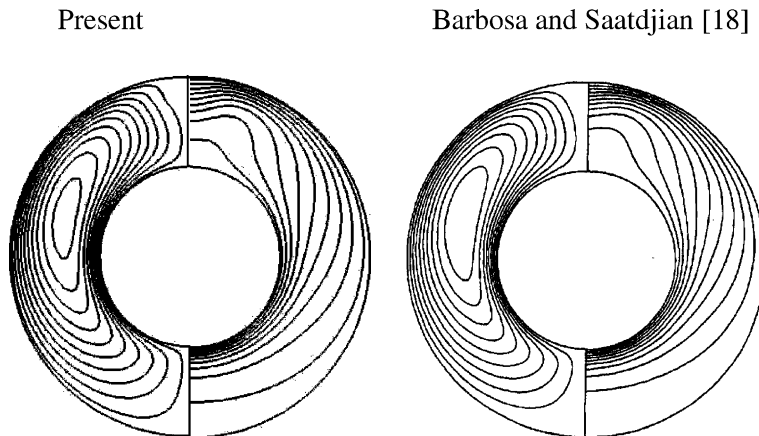


Fig. 4. Comparison of the streamlines and isotherms between the present solution and that of Barbosa and Saadtjian [18] in a porous horizontal cylindrical annulus ( $Ra = 100, R = (R_o/R_i) = 2$ ).

perature except for the density in the buoyancy term, that is, the Boussinesq approximation is invoked. This density variation can be described by the following equation:

$$\rho = \rho_o[1 - \beta(T - T_o)] \quad (1)$$

where  $\beta$  is the coefficient for thermal expansion given by

$$\beta = -\frac{1}{\rho_o} \left( \frac{\partial \rho}{\partial T} \right)_p \quad (2)$$

Taking into consideration the above assumptions and using the following dimensionless parameters

$$R_i = \frac{r_i}{r_o - r_i}, \quad r_o = \frac{r_o}{r_o - r_i}, \quad u = \frac{V}{\omega r_o} \\ \theta = \frac{T - T_o}{T_i - T_o}, \quad P = \frac{p}{\rho_o(\omega r_o)^2} \quad \text{and} \quad \tau = \frac{\omega r_o t}{r_o - r_i}, \quad (3)$$

The governing equations for this investigation can be written in dimensionless form as

$$\nabla \cdot \mathbf{u} = 0 \quad (4)$$

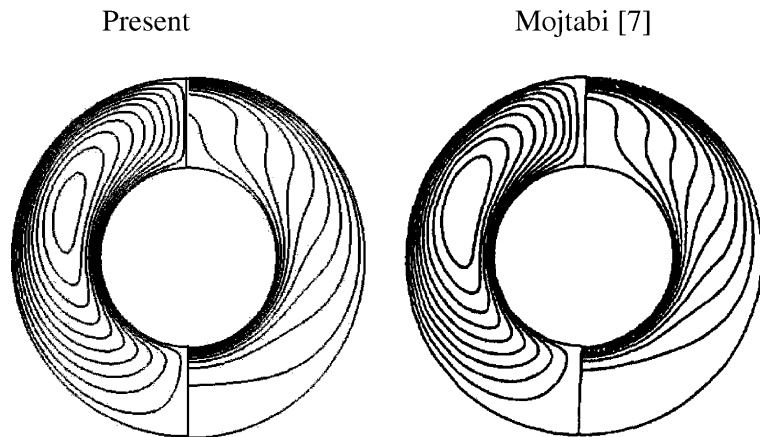


Fig. 5. Comparison of the streamlines and isotherms between the present solution and that of Mojtabi [7] in a porous horizontal cylindrical annulus ( $Ra = 200, R = (R_o/R_i) = 2$ ).

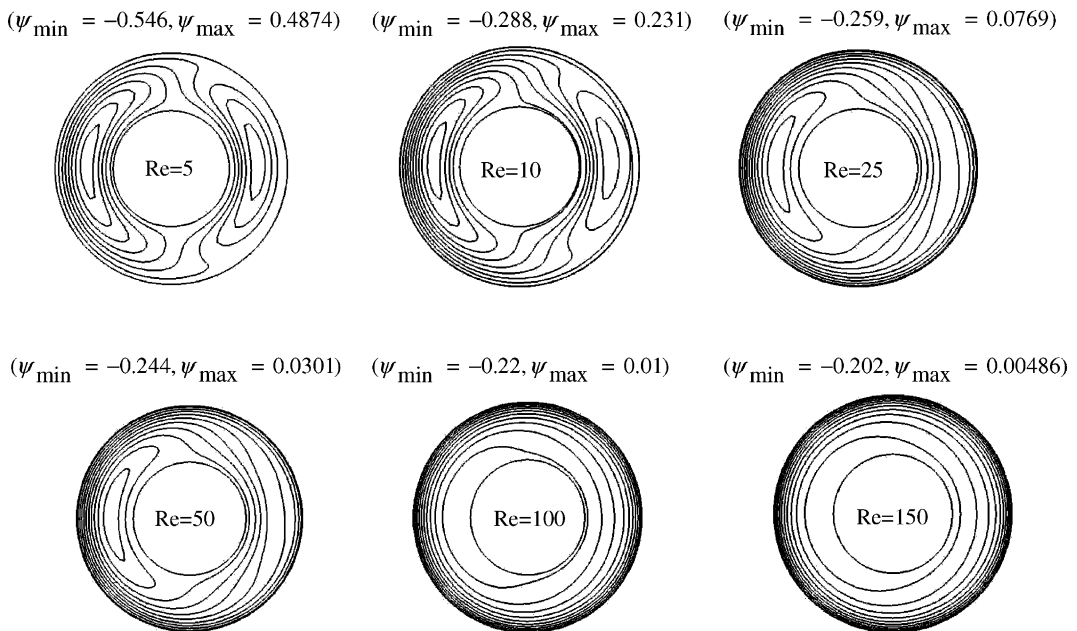


Fig. 6. Effect of the Reynolds number on the streamlines ( $Da = 10^{-1}, Ra = 10^3, Ra_1 = 0$  and  $\sigma = 2$ ).

$$\frac{1}{\varepsilon} \frac{\partial \mathbf{u}}{\partial \tau} = -\nabla P + \frac{\nabla^2 \mathbf{u}}{Re} - \frac{\mathbf{u}}{ReDa} - \frac{F}{\sqrt{Da}} |\mathbf{u}| \mathbf{u} + R_1(\theta \cos \phi e_r - \theta \sin \phi e_\phi) \tag{5}$$

$$\frac{\partial \theta}{\partial \tau} + (\mathbf{u} \cdot \nabla) \theta = \frac{\nabla^2 \theta}{PrRe} + \frac{Ra_1}{Ra} \frac{1}{PrRe} \tag{6}$$

where  $\mathbf{u}$  is the velocity vector  $(u, v)$ ,  $F$  is a function that depends on the Reynolds number and the microstructure of the porous medium [15] and  $\varepsilon$  is the porosity. The nondimensional parameters in the above equations are the Darcy number  $Da$ , the external Rayleigh number  $Ra$ , the internal Rayleigh number  $Ra_1$ , the Richardson number  $R_1$ , the Reynolds number  $Re$ , and the Prandtl number  $Pr$ . These parameters are defined by

$$\left. \begin{aligned} Da &= \frac{\kappa}{(r_o - r_i)^2}, & Ra &= \frac{g\beta(T_i - T_o)(r_o - r_i)^3}{v\alpha} \\ Ra_1 &= \frac{g\beta q'''(r_o - r_i)^5}{v\alpha k}, & Re &= \frac{\omega r_o(r_o - r_i)}{v} \\ R_1 &= \frac{Ra}{PrRe^2}, & Pr &= \frac{v}{\alpha} \end{aligned} \right\} \tag{7}$$

where  $v$  and  $\alpha$  are the fluid kinematic viscosity and the effective thermal diffusivity of the porous medium, respectively. It should be noted that the convective terms in the generalized momentum equation, Eq. (5), are dropped based on the analysis given by Vafai and Tien [15].

The dimensionless form of the initial conditions for the present investigation is given by:

$$u = v = \theta = 0 \quad \text{at } \tau = 0 \tag{8}$$

The dimensionless form of the boundary conditions for the problem is expressed as:

$$u = v = 0, \quad \theta = 1 \quad \text{at } R = R_i \tag{9}$$

$$u = 0, \quad v = 1, \quad \theta = 0 \quad \text{at } R = R_o \tag{10}$$

The local Nusselt numbers along the inner and outer cylinders are calculated as the actual heat transfer divided by the heat transfer in the absence of any fluid motion

$$Nu_i(\phi) = -\left(R \frac{\partial \theta}{\partial R}\right) / Nu_{\text{cond}} = -\ln \frac{R_o}{R_i} \left(R \frac{\partial \theta}{\partial R}\right)_{R=R_i} \tag{11}$$

$$Nu_o(\phi) = -\left(R \frac{\partial \theta}{\partial R}\right) / Nu_{\text{cond}} = -\ln \frac{R_o}{R_i} \left(R \frac{\partial \theta}{\partial R}\right)_{R=R_o} \tag{12}$$

The average Nusselt numbers at the inner and outer cylinders are given, respectively, by

$$\overline{Nu}_i = \frac{1}{2\pi} \int_0^{2\pi} Nu_i(\phi) d\phi \quad \text{and} \tag{13}$$

$$\overline{Nu}_o = \frac{1}{2\pi} \int_0^{2\pi} Nu_o(\phi) d\phi$$

For steady state solutions and in the absence of heat generation, both expressions in Eq. (13) predict the same result. The nondimensional torque acting on the outer cylinder is given by

$$T_r = \int_0^{2\pi} (\tau R^2) d\phi, \quad \tau = R \frac{\partial}{\partial R} \left(\frac{v}{R}\right) \tag{14}$$

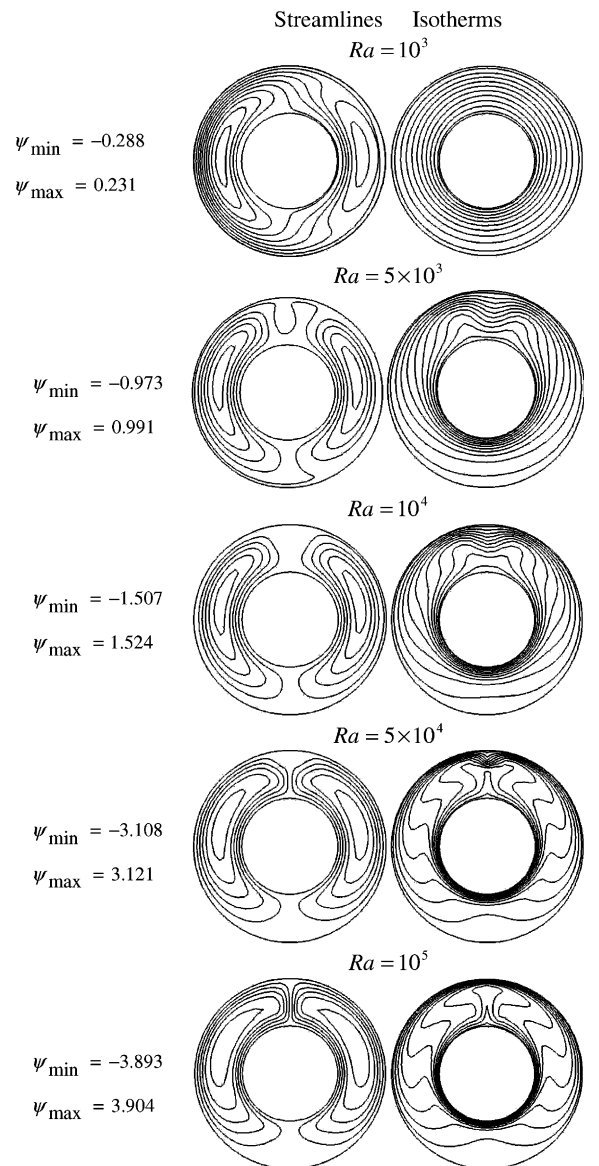


Fig. 7. Effect of the Rayleigh number on the streamlines and isotherms ( $Da = 10^{-1}$ ,  $Ra_1 = 0$ ,  $Re = 10$  and  $\sigma = 2$ ).

### 3. Numerical method

A finite element formulation based on the Galerkin method is employed to solve the governing equations subject to the initial and boundary conditions for the present study. The application of this technique is well described by Taylor and Hood [16] and Gresho et al. [17]. The highly coupled and non-linear algebraic equations resulting from the discretization of the governing equations are solved using an iterative solution scheme using the segregated solution algorithm. The advantage of using this method is that the global system matrix is decomposed into smaller submatrices and then solved in a sequential manner. This technique will result in considerably fewer storage requirements. The conjugate residual scheme is used to solve the symmetric pressure-type equation systems, while the conjugate gradient squared is used for the non-symmetric advection-diffusion-type equations. A variable grid-size system was implemented in the present investigation especially near the walls to capture the rapid changes in the dependent variables. Extensive numerical experimentation was also performed to attain grid-independent results for all the field variables. When the relative change in variables between consecutive iterations was less than  $10^{-5}$ , convergence was assumed to have been achieved.

The validation of the present numerical code is performed against the work of Yoo [6] in the absence of the porous medium and is shown in Fig. 2. It can be seen from this figure that the solution of the present numerical code is in excellent agreement with the numerical results of Yoo [6] for various Reynolds and Rayleigh

numbers. In addition, comparison of the average Nusselt number between the present results and that of Yoo [6] is made as shown in Fig. 3. Both results are found to be in excellent agreement for various Rayleigh and Reynolds numbers. Moreover, the present numerical approach was validated against the works of Barbosa and Saadjan [18] and Mojtabi [7] in a porous horizontal cylindrical annulus for a radius ratio of 2 and Rayleigh numbers of 100 and 200 as shown in Figs. 4 and 5. These comparisons show excellent agreements between the present results and other works available in the literature.

### 4. Results and discussion

A wide range of pertinent parameters such as Reynolds number, Rayleigh number, Darcy number, and the annulus gap width are analyzed in this study. The range of the Reynolds number used in this study was varied between  $5 \leq Re \leq 200$ , Rayleigh number between  $10^3 \leq Ra \leq 10^5$ , internal Rayleigh number between  $0 \leq Ra_1 \leq 10^6$ , Darcy number between  $10^{-6} \leq Da \leq 10^{-1}$ , and the ratio of the inner cylinder diameter to the annulus gap width was taken between  $0.5 \leq \sigma \leq 5$ . Based on the measurements reported by Hunt and Tien [19] for a foam material made of carbon, the porosity of the porous medium was assumed constant ( $\varepsilon = 0.97$ ) and the inertia coefficient was selected to be  $F = 0.1$ .

The effect of the Reynolds number on the streamlines is shown in Fig. 6 for a stagnant outer cylinder and relatively small Rayleigh numbers. For small Reynolds

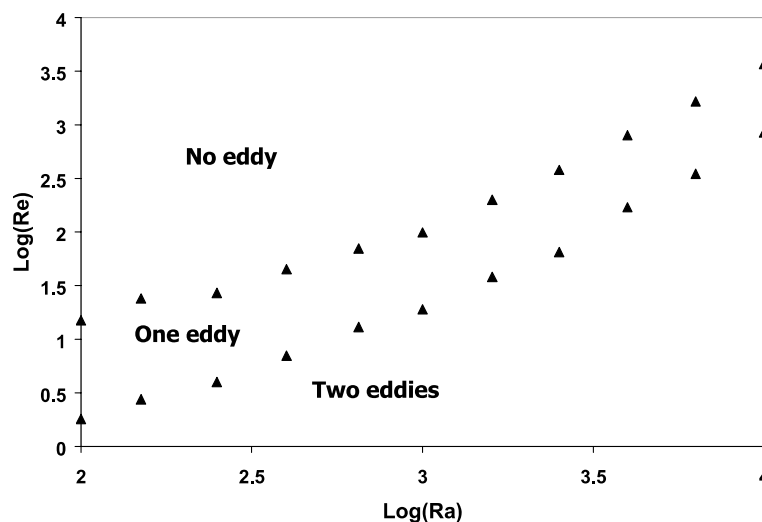


Fig. 8. Categorization of the flow regimes on the  $Ra$ - $Re$  plane for various Rayleigh numbers ( $Da = 0.1$ ,  $Ra_1 = 0$ ,  $\sigma = 2$ ).

numbers the flow field within the annulus is characterized by two symmetric kidney-shaped eddies with respect to the vertical axis as depicted by Kuehn and Goldstein [20]. This pattern in the fluid flow is mainly due to the influence of the buoyancy force. As the Reynolds number increases due to the rotation of the outer cylinder, Fig. 6 illustrates three different flow patterns characterized by two eddies, one eddy, and no eddy depending on the speed of the outer cylinder. Initially as Reynolds number is increased slightly ( $Re = 5$ ),

the symmetry in the flow patterns breaks down and the speed of the eddy in the region of  $\pi \leq \phi \leq 2\pi$  is reduced. An additional increase in the Reynolds number ( $Re = 25$ ) causes the eddy in that region to disappear as a result of strong induced flow by the rotating outer cylinder. This effect becomes more pronounced at higher Reynolds numbers ( $Re = 150$ ) where the remaining eddy in the region  $0 \leq \phi \leq \pi$  disappears. The isotherms are not shown in Fig. 6 since the velocities are too small to affect the temperature distribution at relatively small Reynolds and Rayleigh numbers. Moreover, for higher Reynolds numbers, the isotherms also remain unchanged since the buoyancy force is overwhelmed by the strong influence of the induced flow, which indicates a pure heat transfer by conduction mechanism.

The effect of the Rayleigh number on the streamlines and the isotherms for a Reynolds number of  $Re = 10$  and a Darcy number of  $Da = 10^{-1}$  is shown in Fig. 7. It

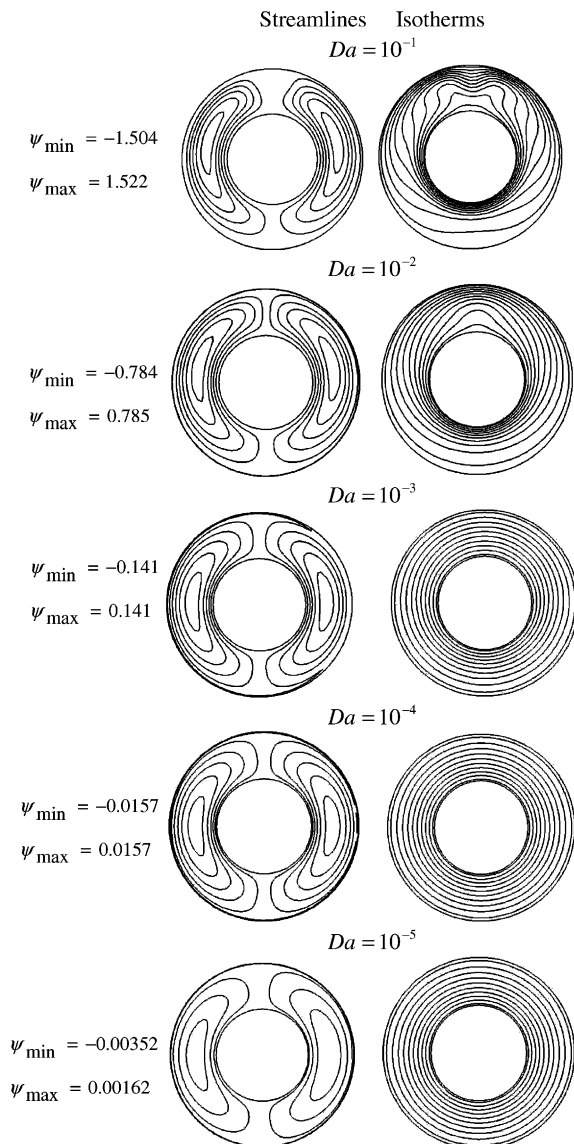


Fig. 9. Effect of the Darcy number on the streamlines and isotherms ( $Ra = 10^4, Ra_1 = 0, Re = 10$  and  $\sigma = 2$ ).

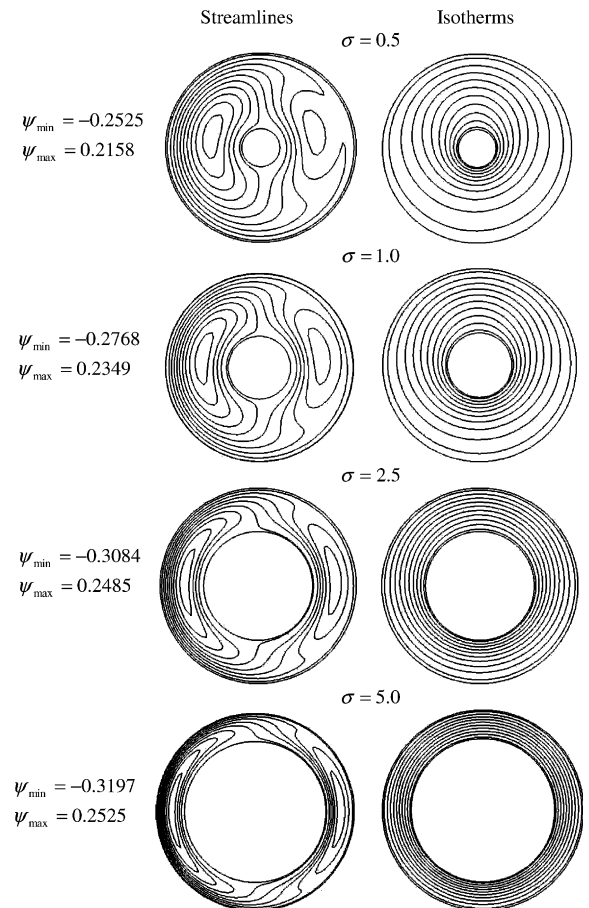


Fig. 10. Effect of the ratio of the inner cylinder diameter to the gap width on the streamlines and isotherms ( $Da = 10^{-1}, Ra = 10^3, Ra_1 = 0$  and  $Re = 10$ ).



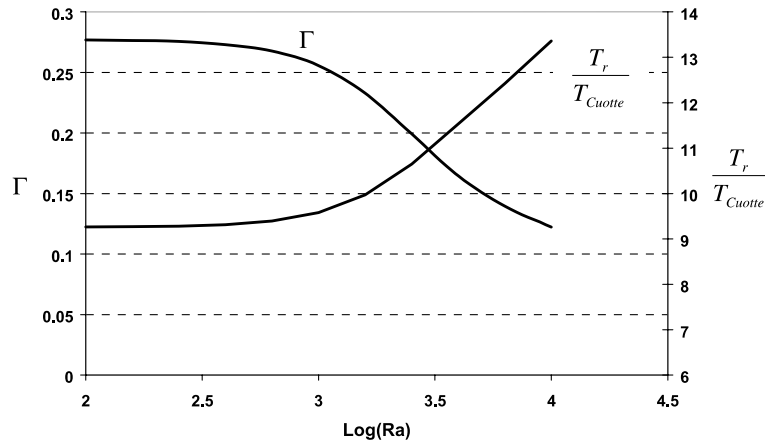


Fig. 11. The effect of Rayleigh number on the net circulation of fluid in the annulus and the normalized torque with respect to Couette flow acting on the outer cylinder ( $Da = 0.1, Ra_1 = 0, Re = 25, \sigma = 2$ ).

can be seen from this figure that as the Rayleigh number increases, the temperature distribution becomes distorted resulting in an increase in the overall heat transfer. This result can be attributed to the dominance of the buoyancy force as compared to the centrifugal force. It is worth noting in Fig. 7 that as the Rayleigh number increases, the thickness of the thermal plume above the inner cylinder increases which indicates a steep temperature gradient and hence an increase in the overall heat transfer within the annulus.

The flow patterns in Figs. 6 and 7 can be categorized into three different patterns namely two eddies, one eddy and no eddy. The classification of the flow regimes according to the number of eddies on the  $Ra-Re$  plane when  $\sigma = 2$  and  $Da = 0.1$  is shown in Fig. 8. This figure gives the transitional Reynolds numbers between different regimes.

The effect of the Darcy number on the streamlines and the isotherms is depicted in Fig. 9. It can be seen from this figure that as the Darcy number decreases, the isotherm pattern change significantly resulting in a pure conduction regime. In this case, isotherms resemble concentric circles for small Darcy numbers. This is due to the bulk damping caused by the presence of the porous matrix. The effect of the Darcy number on the speed of the eddies within the annulus is also depicted in Fig. 9. It is clearly seen in this figure that the velocities within the annulus are substantially decreased except at a very thin zone next to the outer cylinder where the mechanical effect of the rotating outer cylinder is significant. For small values of the Darcy number ( $Da = 10^{-5}$ ), the fluid experiences a pronounced large resistance as it flows through the porous matrix causing the flow to cease in the bulk of the cavity. In this situation, the convective heat transfer mechanism is com-

pletely suppressed indicating a pure conduction regime in the bulk of the annulus.

Fig. 10 illustrates the effect of the ratio of the inner cylinder diameter to the gap width on the streamlines and the isotherms for  $Da = 10^{-1}$ ,  $Ra = 10^3$  and Reynolds numbers of  $Re = 10$ , respectively. It can be shown in this figure that the geometric parameter of the annulus  $\sigma$  significantly alters the fluid flow and the temperature patterns within the annulus. As the ratio of the inner cylinder diameter to the gap width increases, ( $\sigma = 5.0$ ), the fluid has a less space to move within the annulus resulting in a significant decrease in the heat transfer rate. In this case, the isotherms for this case resemble those for the case of pure conduction mechanism within an annulus.

The net circulation of the fluid ( $\Gamma = |\Psi_o - \Psi_i|$ ) in the annulus and the torque normalized with respect to the torque obtained from Couette flow are shown in Fig. 11 for  $Re = 25$ ,  $Da = 0.1$ ,  $\sigma = 2$  and various Rayleigh numbers. This figure shows that as the Rayleigh number increases the net circulation of the fluid in the annulus decreases while the torque acting on the outer cylinder increases due to a strong effect of the natural convection of fluid, which tends to obstruct the circulation of fluid.

The effect of the internal heat generation on the streamlines and the isotherms for  $Da = 0.1$ ,  $Ra = 10^3$ , and a Reynolds number of  $Re = 10$  is shown in Fig. 12. It is seen in this figure that as the internal Rayleigh number increases, the thermal boundary-layer thickness along the outer and inner cylinders decreases thus increasing heat transfer. Moreover, the isotherm plot indicates a localized region of high temperature (relative to the hot wall temperature) between the inner (hot) and the outer (cold) cylinders. The effect of the internal heat generation on the streamlines is also shown in Fig. 12.

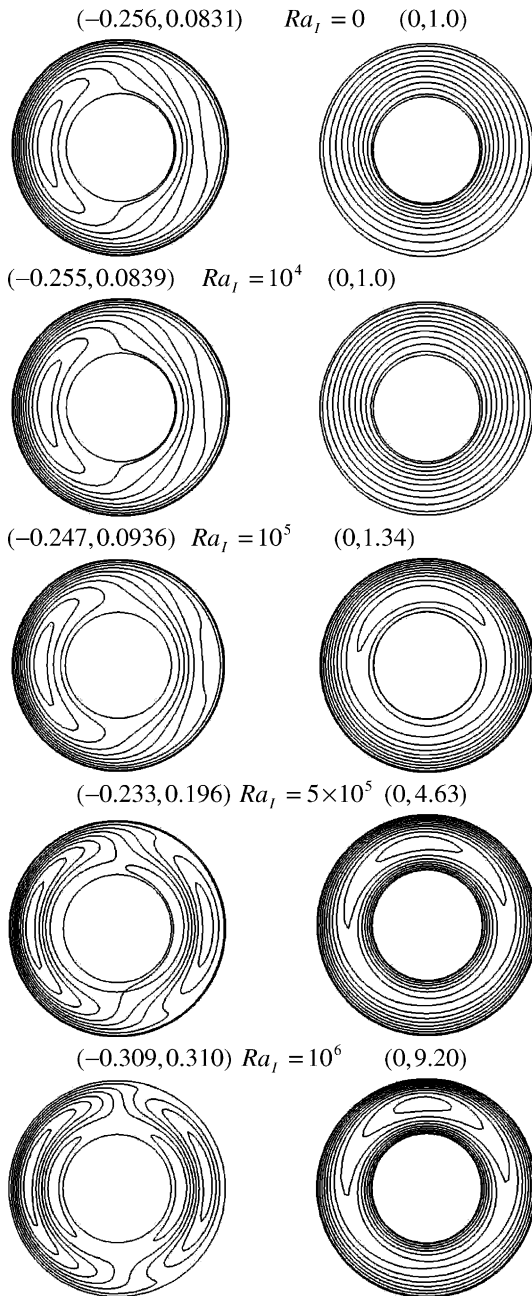


Fig. 12. Effect of the internal Rayleigh number on the streamlines and isotherms ( $Da = 10^{-1}$ ,  $Ra = 10^3$ ,  $Re = 25$ ,  $\varepsilon = 0.97$ ,  $\sigma = 2$ ).

This figure illustrates that the streamlines change significantly at higher internal Rayleigh numbers.

Finally, the influence of the internal Rayleigh number on the average Nusselt numbers along the inner and outer cylinders is shown in Fig. 13. As expected, as the internal Rayleigh number increases, both inner and

outer Nusselt numbers increase. It is worth noting that the outer average Nusselt number is greater than the inner average Nusselt number for all internal Rayleigh numbers.

### 5. Heat transfer correlations

The average Nusselt numbers along the inner cylinder and outer cylinder are correlated in terms of Reynolds number ( $5 \leq Re \leq 200$ ), ratio of the inner cylinder diameter to the gap width ( $0.25 \leq \sigma \leq 5$ ), Rayleigh number ( $10^3 \leq Ra \leq 10^5$ ), Darcy number ( $10^{-6} \leq Da \leq 10^{-1}$ ) and the internal Rayleigh number ( $0 \leq Ra_1 \leq 10^6$ ). These correlations can be expressed as follows

$$\begin{aligned} \overline{Nu}_i = & 1.16985 - 0.13859\sigma + 3.85232Da \\ & - 0.00803Re + 2.301 \times 10^{-5}Ra \\ & + 5.273 \times 10^{-5} \left(\frac{Ra_1}{Ra}\right)^2 - 3.30481 \times 10^{-8} \left(\frac{Ra_1}{Ra}\right)^3 \\ & + 8.8 \times 10^{-6}(\sigma Re)^2 \end{aligned} \quad (15)$$

$$\begin{aligned} \overline{Nu}_o = & 1.02052 - 0.09598\sigma + 3.73308Da - 0.00186Re \\ & + 3.692 \times 10^{-5}Ra_1 + 2.363 \times 10^{-5}Ra \end{aligned} \quad (16)$$

### 6. Conclusions

Mixed convection heat transfer in a two-dimensional horizontal annulus filled with a uniform fluid-saturated porous medium is investigated numerically for a wide range of pertinent parameters. The inner cylinder is heated while the outer cylinder is cooled and rotating at a constant angular velocity. The flow field is modeled using the generalized form of the momentum equation accounting for the viscous, Darcian and the porous medium inertial effects. The present results showed that the Reynolds number has a significant effect on the flow patterns within the annulus with respect to two-eddy, one-eddy and no-eddy flows. Moreover, the obtained results depict that the ratio of the inner cylinder diameter to the gap width plays a significant role on the characterization of the heat transfer mechanism within the porous medium-filled annulus. Categorization of the flow regimes according to the number of eddies is established on the  $Ra-Re$  plane for various Rayleigh numbers. The effect of the Darcy number on the streamlines, isotherms and the heat transfer rates in terms of the average Nusselt number is presented and discussed in this study. The presence of the internal heat

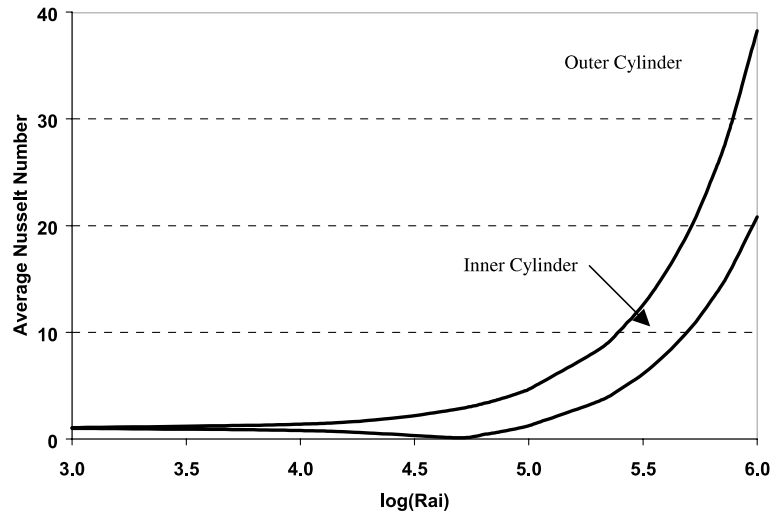


Fig. 13. Effect of the internal Rayleigh number on the average Nusselt number ( $Da = 10^{-1}$ ,  $Ra = 10^3$ ,  $Re = 25$ ,  $\varepsilon = 0.97$ ,  $\sigma = 2$ ).

generation within the annulus is found to play a significant role on the flow patterns and isotherms.

## References

- [1] L. Yang, B. Farouk, Three-dimensional mixed convection flows in a horizontal annulus with a heated rotating inner circular cylinder, *Int. J. Heat Mass Transfer* 35 (1992) 1947–1956.
- [2] R.C. DePrima, H.L. Swinney, Instabilities and transition in flow between concentric rotating cylinders, in: H.L. Swinney, J.P. Gollub (Eds.), *Hydrodynamic Instabilities and the Transition to Turbulence*, Springer, New York, 1985, pp. 139–186.
- [3] T. Fusegi, B. Farouk, K. Ball, Mixed-convection flows within a horizontal concentric annulus with a heated rotating inner cylinder, *Numer. Heat Transfer* 9 (1986) 591–604.
- [4] J.Y. Choi, M. Kim, Three-dimensional linear stability of mixed-convection flow between rotating horizontal concentric cylinders, *Int. J. Heat Mass Transfer* 38 (1995) 275–285.
- [5] T.S. Lee, Numerical experiments with laminar fluid convection between concentric and eccentric heated rotating cylinders, *Numer. Heat Transfer* 7 (1984) 77–87.
- [6] J.S. Yoo, Mixed convection of air between two horizontal concentric cylinders with a cooled rotating outer cylinder, *Int. J. Heat Mass Transfer* 41 (1998) 293–302.
- [7] M.C. Charrier-Mojtabi, Numerical simulation of two- and three-dimensional free convection flows in a horizontal porous annulus using a pressure and temperature formulation, *Int. J. Heat Mass Transfer* 40 (1997) 1521–1533.
- [8] J.P. Caltagirone, *Instabilités thermoconvectives en milieu poreux*, These d'état, Univ. Pierre et Marie Curie, Paris, VI, France, 1976.
- [9] J.P. Caltagirone, Thermoconvective instabilities in a porous medium bounded by two concentric horizontal cylinders, *J. Fluid Mech.* 65 (1976) 337–362.
- [10] J.P. Burns, C.L. Tien, Natural convection in porous media bounded by concentric spheres and horizontal cylinders, *Int. J. Heat Mass Transfer* 22 (1979) 929–939.
- [11] Y.F. Rao, K. Fukuda, S. Hasegawa, Steady and transient analyses of natural convection in a horizontal porous annulus with the Galerkin method, *ASME J. Heat Transfer* 109 (1987) 919–927.
- [12] Y.F. Rao, K. Fukuda, S. Hasegawa, A numerical study of three-dimensional natural convection in a horizontal annulus with a Galerkin method, *Int. J. Heat Mass Transfer* 31 (1988) 695–707.
- [13] I. Pop, D.B. Ingham, P. Cheng, Transient natural convection in a horizontal concentric annulus filled with a porous medium, *ASME J. Heat Transfer* 114 (1992) 990–997.
- [14] W.E. Stewart Jr., A.S. Burns, Convection in a concentric annulus with heat generating porous media and a permeable inner boundary, *Int. Comm. Heat Mass Transfer* 19 (1992) 859–868.
- [15] K. Vafai, C.L. Tien, Boundary and inertia effects on flow and heat transfer in porous media, *Int. J. Heat Mass Transfer* 24 (1981) 195–203.
- [16] C. Taylor, P. Hood, A numerical solution of the Navier–Stokes equations using finite-element technique, *Comput. Fluids* 1 (1973) 73–89.
- [17] P.M. Gresho, R.L. Lee, R.L. Sani, On the time-dependent solution of the incompressible Navier–Stokes equations in two and three dimensions, in: *Recent Advances in Numerical Methods in Fluids*, Pineridge, Swansea, UK, 1980.
- [18] J.P. Barbosa Mota, E. Saadtdjian, Natural convection in a porous horizontal cylindrical annulus, *ASME J. Heat Transfer* 116 (1994) 621–626.
- [19] M.L. Hunt, C.L. Tien, Effects of thermal dispersion on forced convection in fibrous media, *Int. J. Heat Mass Transfer* 31 (1988) 301–310.
- [20] T.H. Kuehn, R.J. Goldstein, An experimental and theoretical study of natural convection in the annulus between horizontal concentric cylinders, *J. Fluid Mech.* 74 (1976) 695–719.